NIH Public Access
Author Manuscript
Cell Metab. Author manuscript; available in PMC 2013 October 03.

Published in final edited form as:
Cell Metab. 2012 October 3; 16(4): 462–472. doi:10.1016/j.cmet.2012.08.011.

Cullin-3 Regulates Vascular Smooth Muscle Function and Arterial Blood Pressure via PPAR γ and RhoA/Rho-kinase

Christopher J. Pelham, **Pimonrat Ketsawatsomkron**, **Séverine Groh**, **Justin L. Grobe**, **Willem J. de Lange**, **Stella-Rita C. Ibeawuchi**, **Henry L. Keen**, **Eric T. Weatherford**, **Frank M. Faraci**, and **Curt D. Sigmund**
Roy J. and Lucille A. Carver College of Medicine, University of Iowa, Iowa City, IA

Summary

Dominant negative mutations in the nuclear hormone receptor peroxisome proliferator-activated receptor-γ (PPARγ) cause hypertension by an unknown mechanism. Hypertension and vascular dysfunction are recapitulated by expression of dominant negative PPARγ specifically in vascular smooth muscle of transgenic mice. Dominant negative PPARγ increases RhoA and Rho-kinase activity, and inhibition of Rho-kinase restores normal reactivity and reduces arterial pressure. RhoBTB1, a component of the Cullin-3 RING E3 ubiquitin ligase complex, is a PPARγ target gene. Decreased RhoBTB1, Cullin-3 and neddylated Cullin-3 correlated with increased levels of the Cullin-3 substrate RhoA. Knockdown of Cullin-3 or inhibition of cullin-RING ligase activity in aortic smooth muscle cells increased RhoA. Cullin-RING ligase inhibition enhanced agonist-mediated contraction in aortic rings from normal mice by a Rho-kinase-dependent mechanism, and increased arterial pressure *in vivo*. We conclude that Cullin-3 regulates vascular function and arterial pressure thus providing a mechanistic link between mutations in Cullin-3 and hypertension in humans.

Introduction

PPARγ is activated by thiazolidinediones (TZDs), a class of insulin-sensitizing drugs. TZD treatment attenuates the development of hypertension and inhibits atherosclerosis in type II diabetes patients (Halabi and Sigmund, 2005). Known adverse effects of TZD treatment include weight gain and systemic edema. Clinical studies report an increased risk of myocardial infarction and heart failure in patients taking the TZD rosiglitazone (Graham et al., 2010); and more recently, concerns of increased risk of bladder cancer have surfaced with pioglitazone (Lewis et al., 2011). TZDs increase water and salt retention by the kidneys, yet their use consistently lowers blood pressure, suggesting that the anti-hypertensive effects of tissue-specific PPARγ activation in non-renal tissues are potent (Ketsawatsomkron et al., 2010). While PPARγ is well characterized as a master regulator of adipogenesis, the direct actions of PPARγ within the vasculature remain unclear. Given the concerns over TZD use, understanding the fundamental mechanisms of PPARγ action in

© 2012 Elsevier Inc. All rights reserved.

Corresponding Author: Curt D. Sigmund, Ph.D., Department of Pharmacology, Roy J. and Lucille A. Carver College of Medicine, University of Iowa, 375 Newton Rd., 3181 MERF, Iowa City, Iowa, 52242, Phone: 319-335-7604, Fax: 319-353-5350, curt-sigmund@uiowa.edu.

Disclosures: None.

Publisher's Disclaimer: This is a PDF file of an unedited manuscript that has been accepted for publication. As a service to our customers we are providing this early version of the manuscript. The manuscript will undergo copyediting, typesetting, and review of the resulting proof before it is published in its final citable form. Please note that during the production process errors may be discovered which could affect the content, and all legal disclaimers that apply to the journal pertain.

NIH-PA Author Manuscript
NIH-PA Author Manuscript
NIH-PA Author Manuscript

NIH-PA Author Manuscript

NIH-PA Author Manuscript

NIH-PA Author Manuscript

specific tissues is essential in order to identify therapeutic pathways that promote the beneficial actions of PPARγ while minimizing detrimental actions. A new class of non-TZD ligands that prevent Cyclin-dependent kinase 5 (Cdk5)-dependent inhibition of PPARγ and lack agonist activity may provide a similar level of glycemic control as TZD but without adverse effects on weight gain and fluid retention (Choi et al., 2011).

Individuals carrying mutations (i.e. P467L, V290M) and knock-in mice with an equivalent mutation (P465L) in PPARγ develop early-onset hypertension (Barroso et al., 1999; Tsai et al., 2004). Mutation of the ligand-binding domain of PPARγ prevents ligand activation, but retains its ability to bind DNA and complex with co-repressors. Thus, these mutations confer dominant negative (DN) activity, which alters PPARγ-mediated transcription (Li and Leff, 2007). We demonstrated that smooth muscle cell-targeted expression of DN human PPARγ in transgenic mice (termed S-P467L) caused elevated blood pressure and vascular dysfunction independent of changes in systemic metabolism (Halabi et al., 2008). This and other studies employing vascular-specific knockout of PPARγ are consistent with the hypothesis that PPARγ activation exerts its antihypertensive and vascular protective effects through actions in vascular endothelium and smooth muscle. Therefore, the aim of the current study is to elucidate the molecular mechanisms that underlie augmented contraction and impaired relaxation induced by expression of DN PPARγ in smooth muscle.

Results

Dominant Negative PPARγ-Induced Aortic Dysfunction is Smooth Muscle-Specific

Smooth muscle-specific expression of dominant negative (DN) PPARγ in S-P467L mice caused severely impaired relaxation to Ach and SNP (Figure 1A). Pre-incubation of aortic rings with L-NAME or removal of the endothelium completely abrogated Ach-induced relaxation in both S-P467L and NT but had no effect on SNP-induced relaxation (Figure 1A, Figure S1A). The impairment in vasodilation is not due to increased superoxide because pre-incubation with Tempol, a scavenger of superoxide, did not alter the responses to either Ach or SNP (Figure S1B). The level of total and phospho-Ser^{1177} eNOS protein was similar in aortic tissue from NT and S-P467L mice (Figure S1C). ET-1 and 5-HT caused enhanced contraction of S-P467L aorta which was augmented by either NOS inhibition or removal of the endothelium (Figures 1B and S1D-E). As above, pre-treatment with Tempol had no effect on agonist-induced contraction (Figure S1F). These data suggest that NO production and bioavailability is unaltered and that aortic dysfunction in S-P467L mice is due to some other mechanism.

Dominant Negative PPARγ Increases Rho-kinase Activity

We tested the hypothesis that the RhoA/Rho-kinase pathway is a downstream target of PPARγ and that enhanced activation of Rho-kinase limits the effectiveness of NO/PKG signaling in S-P467L (Chitaley and Webb, 2002). Basal Rho-kinase activity, measured by Thr^{696} phosphorylation of the myosin light chain phosphatase subunit MYPT1, was significantly increased in lysates from S-P467L aorta (Figure 1C). The increase in Rho-kinase activity was inhibited by Y-27632, a specific inhibitor of both Rho-kinase isoforms ROCK1 and ROCK2 (Figure 1C). Consistent with this, pre-incubation of aortic rings with Y-27632 blunted the hypercontractile responses from S-P467L aorta (Figures 1D and S2A), thus demonstrating that the enhanced contraction is Rho-kinase-dependent. Importantly, pre-incubation with Y-27632 fully restored NO-mediated dilator responses in S-P467L aorta (Figure 1E). The improvement in Ach-induced relaxation after Rho-kinase blockade in S-P467L aorta was abrogated by NOS inhibition or endothelium removal indicating it is endothelium-dependent (Figure S2B). This suggests that increased activity of the Rho-kinase pathway in smooth muscle is responsible for the DN PPARγ-induced defect in NO-

NIH-PA Author Manuscript

NIH-PA Author Manuscript

NIH-PA Author Manuscript

mediated relaxation. Likewise, intravenous injection of Y-27632 decreased mean arterial pressure by 30±3 mmHg in S-P467L mice compared with 16±1 mmHg ($p<0.05$) in NT mice (Figure 1F), strongly suggesting the increase in arterial pressure caused by DN PPARγ is Rho-kinase-dependent.

Because Rho-kinase enhances the sensitivity of the contractile apparatus to Ca^{2+}, we tested if contraction to $CaCl_2$ was enhanced in ionomycin-permeabilized aortic rings. Aorta from S-P467L mice displayed increased contraction at lower concentrations of $CaCl_2$ compared to NT mice (S-P467L EC_{50} = 4.3 mmol/L vs. NT EC_{50} = 22.1 mmol/L; $p<0.05$) while maximum contraction was not different (Figure S2C). Similar to receptor-mediated agonists, Bay K8644 augmented contraction in S-P467L aorta that was both NO- and Rho-kinase-dependent (Figure S2D). On the contrary, the PKC activator phorbol 12,13-dibutyrate (PdBu) produced contraction that was similar between NT and S-P467L aorta and was not sensitive to L-NAME nor Y-27632 pre-incubation (Figure S2E).

Dominant Negative PPARγ Increases RhoA Protein and Activity

The mechanism for increased Rho-kinase activity was not due to a change in the protein levels of ROCK1 and ROCK2 (Figure 2A). On the contrary, the protein level of RhoA GTPase, which lies upstream and is a primary regulator of Rho-kinase, was increased in entire aorta from S-P467L mice under baseline conditions (Figure 2A). Despite this, the level of RhoA mRNA was unchanged in S-P467L aorta (Figure 2B). ROCK1 and ROCK2 mRNA levels were also unchanged (Figure 2B). The increase in RhoA is specific to the smooth muscle since RhoA protein was increased in medial aortic tissue (e.g. dissected free of endothelium and adventitia) and in primary aortic smooth muscle cells from S-P467L mice (Figure 2C). Increased total RhoA protein correlated with a greater basal level of active GTP-bound RhoA in primary aortic smooth muscle cells from S-P467L. Next, we determined the levels of GTP-bound RhoGTPases in basal or agonist-stimulated aortic rings equilibrated to resting tension (0.5 g). While the basal level of RhoA-GTP was not different between S-P467L and NT aortic rings at resting tension, 5-HT stimulation significantly increased RhoA-GTP to a greater extent in S-P467L aorta (Figure 2D). 5-HT produced the maximal difference in contraction between genotypes (Figure S1D-F) and it induces GTP-bound RhoA (Sakurada et al., 2001). The level of GTP-bound Rac1 was unaffected by 5-HT stimulation and was not different between genotypes (Figure S3A). GTP-bound Cdc42 was not detected in the basal or stimulated state, but could be detected in control lysates incubated with GTPγS (Figure S3B). Like RhoA, Rac1 and Cdc42 mRNA was unchanged in S-P467L aorta (Figure S3C). These data suggest that interference with PPARγ in smooth muscle leads to enhanced Rho-kinase activity via increased expression and activity of its upstream regulator RhoA.

PPARγ Regulates RhoBTB1 Expression

To gather insights into the molecular mechanism for the increase in RhoA/Rho-kinase activity, we performed gene expression profiling on aorta from NT and S-P467L mice by employing both oligonucleotide and exon tiling arrays. Numerous PPARγ target genes related to lipid metabolism were downregulated by DN PPARγ in the aorta of S-P467L mice, consistent with PPARγ's role as a major regulator of adipogenesis. However, we focused on RhoBTB1, which was markedly decreased (Figure 3A), because it has previously been implicated to bind to Cullin-3 (Berthold et al., 2008), a cullin-RING E3 ubiquitin ligase complex scaffold protein which regulates the turnover of RhoA (Chen et al., 2009). RhoBTB1 mRNA and protein was decreased by approximately 72% and 34% as confirmed by real time quantitative RT-PCR (Figure 3A) and Western blot (Figure 3B), respectively. Evidence suggesting RhoBTB1 is a PPARγ target gene was three-fold. First, expression of RhoBTB1 protein was increased in aorta from transgenic mice over-

NIH-PA Author Manuscript

NIH-PA Author Manuscript

NIH-PA Author Manuscript

expressing wild type PPARγ in smooth muscle (S-WT mice, Figure 3B). Second, PPARγ and retinoid X receptor (RXR) binding sites were detected at the RhoBTB1 locus by genome wide chromatin immunoprecipitation (ChIP, Figure S4A). Third, we validated PPARγ binding at the RhoBTB1 locus using ChIP in differentiated 3T3-L1 cells (Figure 3C). Cullin-3 is known to interact with many BTB domain-containing proteins, including RhoBTBs, which may act as substrate adaptors and/or direct substrates of Cullin-3-dependent ubiquitylation (Berthold et al., 2008). Reciprocal IP, employing Flag-tagged Cullin-3 and Myc-tagged RhoBTB1 co-expressed in HEK293T cells, revealed direct interaction between RhoBTB1 and Cullin-3 that was not affected by proteasome inhibition (Figure 3D).

Dominant Negative PPARγ Impairs Cullin-3

The increase in total RhoA protein, but not mRNA, coupled with decreased RhoBTB1 suggested the hypothesis that DN PPARγ in smooth muscle interferes with Cullin-3-mediated post-translational regulation of RhoA. Cullin-3 protein and the ratio of neddylated Cullin-3 to unneddylated Cullin-3 was decreased in aorta from S-P467L mice (Figure 4A–B). The covalent attachment of Nedd8, called neddylation, is required for cullin-dependent ubiquitin ligase activity (Wu et al., 2005). Total Nedd8-conjugates were detected only at the molecular weight corresponding to neddylated cullins (~90–95 kDa), whereas free monomeric Nedd8 (~8 kDa) was not detected. That there were no changes in the levels of Cullin-1, neddylated Cullin-1 or total Nedd8-conjugates in S-P467L aorta suggests the defect is specific to Cullin-3 (Figure 4A–B). Cullin-3 mRNA was not different between NT and S-P467L aorta (Figure 4B). The identity of the neddylated forms of cullins was confirmed by using the Nedd8-activating enzyme inhibitor MLN4924. Although there are no Cullin-specific (Cul1, 2, 3, 4A, 4B, 5, 7, 9) inhibitors, MLN4924 treatment effectively decreases the levels of neddylated cullins in human and mouse tissues (Soucy et al., 2009). Treatment of primary rat aortic smooth muscle cells with MLN4924 eliminated the presence of neddylated Cullin-3, neddylated Cullin-1 and total Nedd8-conjugates (Figure 4C–D). MLN4924 treatment also increased levels of RhoA, a Cullin-3 substrate (Figure 4C–D).

Cullin-3 Mediates RhoA Turnover in Smooth Muscle

To determine if the decrease in Cullin-3 is mechanistically related to the increase in RhoA protein in S-P467L aorta, we performed siRNA-mediated knockdown of Cullin-3 in primary rat aortic smooth muscle cells. There was no effect of negative control NC1 siRNA whereas two different siRNAs directed against Cullin-3 decreased its expression by nearly 85% (Figure 5A). Loss of Cullin-3 expression caused a robust increase in RhoA and interestingly also increased levels of RhoBTB1 (Figure 5B). This suggests that RhoBTB1 is a substrate of Cullin-3-mediated degradation and explains why the level of RhoBTB1 protein was only modestly decreased in S-P467L aorta. Cyclin E, another substrate of Cullin-3-mediated degradation (Kossatz et al., 2010), was also increased by siRNA-mediated Cullin-3 knockdown in cells (Figure 5B) and in S-P467L aorta (data not shown). siRNA-mediated knockdown of RhoBTB1 in primary rat aortic smooth muscle cells caused a modest yet significant decrease in Cullin-3 and neddylated Cullin-3 protein and a trend toward increased RhoA, but this was not as dramatic as Cullin-3 knockdown (Figure S4B). Interestingly, analysis of both oligonucleotide and exon microarrays revealed no changes in the level of mRNA encoding proteins involved in neddylation and BTB-domain containing proteins other than RhoBTB1 (Table S1).

cullin-RING ligase activity regulates vascular function and blood pressure

We next tested the hypothesis that inhibition of cullin-RING ligase activity leads to enhanced contraction. We established above that RhoA protein levels were robustly upregulated by 16 hr after treatment with MLN4924 (Figure 4C–D). Therefore, aortic rings

NIH-PA Author Manuscript

NIH-PA Author Manuscript

NIH-PA Author Manuscript

from NT mice were first incubated for 16 hr *ex vivo* with MLN4924 or vehicle and then isometric tension studies were performed in the presence of the inhibitor. MLN4924 enhanced agonist-induced contraction to ET-1, 5-HT and PE in NT aorta, despite blunting receptor-independent contraction to KCl (Figure 6A–D). Pre-incubation with the Rho-kinase inhibitor Y-27632 was effective at blocking the MLN4924-dependent enhanced contractile responses (Figure 6A–D). Acute treatment of the vessels with MLN4924 for only 1 hr was not sufficient to alter reactivity, whereas long-term treatment of aortic rings from NT mice *ex vivo* with MLN4924 for 6 days produced the same results as 16 hr (data not shown). We next tested if the enhanced agonist-induced contraction in S-P467L mice was occurring through this mechanism. Consistent with a loss of Cullin-3 mediated activity, the effect of MLN4924 was markedly blunted in S-P467L aorta (Figure 6E–H). Together these data show that inhibition of cullin-RING ligase activity causes striking alterations in vascular contractility, likely in part, through loss of Cullin-3-mediated regulation of RhoA/Rho-kinase signaling.

Finally, to provide an *in vivo* correlate to the vascular function experiments, we measured arterial pressure by radiotelemetry in conscious NT and S-P467L mice in response to MLN4924 using a previously established dose regimen (Soucy et al., 2009; Smith et al., 2012). Compared to baseline, continuous administration of MLN4924 (subcutaneous injections; 30 mg/kg TID, 2.5 days) caused a significant increase in daytime arterial pressure in normal NT mice (Figure 7A and S5). Baseline arterial pressure was significantly higher in S-P467L mice, but MLN4924 treatment did not raise arterial pressure further. MLN4924 treatment caused a marked decrease in spontaneous activity during the nighttime hours (Figure 7B) that was equivalent in both NT and S-P467L mice. The decrease in activity correlated to a loss of normal diurnal variation in arterial pressure and heart rate that was also independent of genotype (Figure 7A–C). MLN4924 administration significantly reduced the level of neddylated Cullin-3 and total Nedd8-conjugates and increased RhoA protein in aortic tissue from NT mice (Figure 7D). These data suggest that cullin-RING ligase activity may be important for blood pressure regulation, and are consistent with the hypothesis that loss of Cullin-3 in the vasculature contributes to hypertension. Indeed, mutations in Cullin-3 cause severe early-onset hypertension (Boyden et al., 2012), although the tissue-specific actions of Cullin-3 remain unclear. The hypertension in patients harboring Cullin-3 mutations was associated with changes in ion homeostasis, namely potassium and bicarbonate balance (Boyden et al., 2012). Blood electrolytes, except for decreased blood urea nitrogen (BUN), were normal in untreated S-P467L mice compared to NT mice (Table S2). Systemic MLN4924 treatment caused mild hyperkalemia, decreased hematocrit and increased BUN that was also not specific to genotype (Table S2).

Discussion

PPARγ within the vascular wall has a pivotal role in protecting against vascular dysfunction or abnormal vascular growth and remodeling during hypertension (Diep et al., 2002); however, the mechanisms behind such improvements remain unclear. PPAR/RXR heterodimers, bound to corepressors, actively silence transcription at PPAR response elements (PPREs). Ligand activation stimulates coactivators to replace corepressors and allow transcription of target genes (Gronemeyer et al., 2004). Interestingly, genetic deletion of PPARγ causes induction of some genes due to loss of PPAR-dependent active repression, which may mimic PPARγ activation (Chang et al., 2009; Sigmund, 2010). Our approach was guided by the identification of *bona fide* mutations in the PPARγ ligand-binding domain from patients who developed early-onset hypertension and insulin resistance (Barroso et al., 1999; Savage et al., 2003). Mice homozygous for the equivalent PPARγ P465L knock-in mutation die *in utero*, confirming that the DN mutation is detrimental to receptor function (Tsai et al., 2004). PPARγ P465L heterozygous (P465L/+) mice develop

NIH-PA Author Manuscript

NIH-PA Author Manuscript

NIH-PA Author Manuscript

hypertension and features of metabolic syndrome (Tsai et al., 2004). Global gene expression analysis validated that PPARγ target genes induced by agonist treatment were also repressed by DN PPARγ in vascular tissue (Keen et al., 2010; Keen et al., 2004). Herein, we combined physiological, biochemical and bioinformatic approaches to identify PPARγ target genes that regulate vascular function and arterial pressure.

The mechanisms contributing to vascular dysfunction induced by smooth muscle-specific expression of DN PPARγ are as follows: 1) endothelium-dependent production of NO is preserved; 2) enhanced Rho-kinase activity is responsible for increased agonist-induced contraction, impaired NO-mediated relaxation, and increased arterial pressure in S-P467L mice; 3) increased RhoA protein and RhoA-GTP upstream of Rho-kinase results from impaired Cullin-3-mediated RhoA turnover in vascular muscle; 4) RhoBTB1, which interacts with Cullin-3, is a PPARγ target gene and is downregulated by DN PPARγ in vascular muscle; 5) pharmacological inhibition of cullin-RING ligase activity in aortic segments from wild type mice causes augmented agonist-induced contraction that is Rho-kinase-dependent; and 6) inhibition of cullin-RING ligase activity in wild type mice *in vivo* causes increased daytime arterial pressure.

Increased RhoA/Rho-kinase activity is implicated in the pathogenesis of many cardiovascular diseases although the underlying causes are not well understood (Budzyn et al., 2006). Basal release of NO from the endothelium prevents activation of RhoA/Rho-kinase in smooth muscle through PKG-dependent inhibitory phosphorylation of RhoA (Sauzeau et al., 2000). Excessive reactive oxygen species (ROS; e.g. superoxide) inactivate NO, leading to a reduction of NO bioavailability and increased vascular tone, at least in part, through elevated RhoA/Rho-kinase activity (Jin et al., 2006). However, our results suggest that increased activation of Rho-kinase in S-P467L aorta is neither a result of oxidative stress nor decreased bioavailability of endothelium-derived NO but is most likely due to a primary defect in the smooth muscle. This is consistent with the genetic lesion being targeted to the smooth muscle.

We next sought to determine the primary PPARγ-dependent effect on regulators upstream of Rho-kinase. The dual regulation of MLC phosphorylation through Ca^{2+}-dependent activation of MLCK and RhoA/Rho-kinase-dependent inhibition of MLCP is attributed to the coupling of G protein coupled receptors (GPCRs) to $G\alpha_{q/11}$ and $G\alpha_{12/13}$, respectively (Maguire and Davenport, 2005; Wirth et al., 2008). Stimulation of aortic smooth muscle cells with agonists of GPCRs including ET-1, 5-HT and PE, in addition to high KCl, enhances RhoA-GTP, which activates Rho-kinase (Sakurada et al., 2003; Sakurada et al., 2001; Momotani et al., 2011). We provide clear evidence of increased RhoA protein, RhoA-GTP and Rho-kinase activity in S-P467L aorta. Thus, PPARγ-dependent regulation of the RhoA/Rho-kinase and NO/PKG-dependent signaling in smooth muscle is key in shifting the balance between vasoconstrictor and vasodilator responses. The PPARγ agonist pioglitazone was shown to lower systolic blood pressure and suppress RhoA/Rho-kinase activity in aortic tissue of spontaneously hypertensive rats (SHR) (Wakino et al., 2004). Similarly, up-regulation of RhoA in Dahl salt-sensitive hypertensive rats was decreased by telmisartan, a dual ARB/PPARγ agonist (Kobayashi et al., 2008). Whereas reports have demonstrated that activation of PPARγ with TZDs suppresses RhoA/Rho-kinase signaling in microvascular endothelial cells (Ramirez et al., 2008), monocytes (Toriumi et al., 2003), and neurons (Dill et al., 2010), the mechanisms are not established.

Expression of DN PPARγ in smooth muscle of S-P467L mice caused increased RhoA protein level in the aorta; however, this was not associated with a change in RhoA mRNA, suggesting a potential alteration in post-translational regulation of RhoA. This was supported by gene expression profiling revealing a marked decrease in RhoBTB1, an

NIH-PA Author Manuscript

NIH-PA Author Manuscript

NIH-PA Author Manuscript

atypical Rho GTPase which lacks GTPase activity. RhoBTB1 binds to the N-terminal region of Cullin-3 through its BTB domain (Berthold et al., 2008). RhoA is a substrate targeted by the Cullin-3 E3 RING ubiquitin ligase complex for ubiquitylation and subsequent degradation in the proteasome (Chen et al., 2009). Silencing of human Cullin-3 caused a loss of RhoA ubiquitylation, accumulation of RhoA protein and RhoA-GTP, and induced actin stress fiber formation that was RhoA-dependent in Hela cells (Chen et al., 2009). We found decreased levels of Cullin-3 and neddylated Cullin-3 in aorta from S-P467L mice. The decreased ratio of Nedd8-conjugated Cullin-3 to unneddylated Cullin-3 is important because the neddylation of cullins is required for cullin-RING ubiquitin ligase activity (Petroski and Deshaies, 2005). Our data support that loss of Cullin-3 in primary rat aortic smooth muscle cells causes accumulation of its substrates, including RhoA and Cyclin E, and raised the possibility that inhibition of Cullin-3 activity may regulate vascular reactivity. To test this, we used MLN4924, an inhibitor of Nedd8-activating enzyme, which catalyzes Nedd8 conjugation onto cullins (Soucy et al., 2009). MLN4924 treatment blocked neddylation of Cullin-3 and Cullin-1 and completely blocked the formation of total Nedd8-conjugates in primary rat aortic smooth muscle cells. This suggests a remarkable specificity of Nedd8 conjugation onto cullins in vascular tissue. Treatment of aorta from wild-type (NT control) mice with MLN4924 caused increased agonist-induced contraction that, despite the broad effects of cullin inhibition, was Rho-kinase-dependent. This is consistent with studies reporting that MLN4924 treatment of HEK293 cells caused accumulation of RhoA protein and altered cell morphology that was completely reversed by siRNA-knockdown of RhoA (Leck et al., 2010). Our *in vivo* studies revealed that systemic administration of NT mice with MLN4924 caused a significant increase in arterial pressure, at least during the light phase, whereas its administration to S-P467L mice did not. This supports our conclusion that the impairment of Cullin-3-mediated regulation of RhoA in the vasculature contributes to hypertension. Systemic MLN4924 treatment also had non-specific effects on the normal diurnal variation in arterial pressure, heart rate and activity. Consequently, use of gene-targeted mice would better clarify the actions of specific cullins in the blood vessel.

Cullin-based E3 ubiquitin ligases are dimeric and Cullin-3/substrate homooligomers are dependent on substrate dimer formation (Chew et al., 2007). Cullin-3 is the only cullin-RING ligase member reported to bind to BTB domain-containing proteins for its substrate specificity (Petroski and Deshaies, 2005). The finding that RhoBTB1 is a PPARγ target gene downregulated by DN PPARγ in S-P467L aorta was instrumental in discovering the accompanying decrease in Cullin-3, and suggests that RhoBTB1 may regulate Cullin-3 level or activity. It has been hypothesized that RhoBTBs may regulate the targeting of specific Cullin-3 substrates, including RhoA. This is based on the observation that RhoBTB1 and RhoBTB2 are candidate tumor suppressors and their loss correlates with increased RhoA protein in breast and head and neck cancers (Beder et al., 2006; Nethe and Hordijk, 2010). Our results from siRNA knockdown of RhoBTB1 suggest that its downregulation partially explains decreased Cullin-3 levels indicating perhaps some other PPARγ-dependent or PPARγ-independent effects are involved in this mechanism. Some candidates are BTB domain-containing RhoA binding proteins (BACURDs), which were recently identified to be adaptors for Cullin-3 mediated RhoA ubiquitylation (Chen et al., 2009). Expression of BACURDs, at least at the mRNA level, did not appear to be regulated by PPARγ in vascular muscle on the basis of our microarray data (Table S1). Identifying which adaptor proteins control substrate specificity for Cullin-3 remains under active investigation, and new substrates for Cullin-3:RhoBTB-domain-mediated ubiquitylation continue to be uncovered (Schenkova et al., 2012). Additional investigation will be required to determine the full range of substrates the RhoBTB family of proteins anchor to Cullin-3.

A role for Cullin-3 in hypertension has recently been reported (Boyden et al., 2012). Remarkably, greater than 90% of patients with dominant mutations in *cullin-3* developed

NIH-PA Author Manuscript

NIH-PA Author Manuscript

NIH-PA Author Manuscript

hypertension before the age of 18, as did about 15% of patients with mutations in *KLHL3*, a Cullin-3 substrate adaptor. The mutations were discovered from a group of patients with pseudohypoaldosteronism type II (PHAII), a syndrome characterized by hypertension, hyperkalemia and metabolic acidosis. Our data indicate that hypertension caused by smooth muscle-specific expression of DN PPARγ in S-P467L transgenic mice is not related to changes in electrolyte balance. Patients with DN mutations in PPARγ also develop early-onset hypertension but have normal serum potassium levels (Savage et al., 2003). In PHAII, *cullin-3* mutations may not only perturb renal ion transport as demonstrated for mutations in one of its partners *KLHL3* (Louis-dit-Picard et al. 2012), but perhaps may also provoke a severe and early-onset hypertension (Boyden et al. 2012) by increasing vascular contraction and impairing the response to NO. Together these findings lead to the hypothesis that hypertension caused by *cullin-3* mutations may be due in part to impaired Cullin-3 mediated regulation of RhoA/Rho- kinase in vascular smooth muscle. We conclude that interference with PPARγ signaling, either through mutation or perhaps through inhibitory modification (i.e. Cdk5-mediated phosphorylation at serine 273) (Choi et al., 2011), causes a decrease in Cullin-3 activity associated with loss of the Cullin-3 interacting protein RhoBTB1. Impaired Cullin-3-dependent degradation of RhoA results in enhanced RhoA/Rho-kinase signaling and causes an imbalance in responsiveness to vasodilator and vasoconstrictor signals leading to hypertension. Hence, under normal conditions PPARγ facilitates tight regulation of RhoA/Rho-kinase activity via Cullin-3-mediated turnover of RhoA. Future studies are needed to discern the extent that aberrant regulation of Cullin-3 activity or expression in the vasculature and other tissues contributes to hypertension and cardiovascular disease.

Experimental Procedures

Transgenic Mouse Model

S-P467L transgenic mice were described previously and were backcross bred to C57BL/6J for at least 10 generations (Halabi et al., 2008). All mice were fed standard mouse chow (7013, Teklad Premier Laboratory Diets) and water ad libitum. Care of the mice used in the experiments met the standards set forth by the National Institutes of Health (NIH) guidelines for the care and use of experimental animals. All procedures were approved by the University of Iowa Institutional Animal Care and Use Committee.

Wire Myograph Preparation

Isometric tension was measured on aorta from mice 5–6 months of age as reported (Halabi et al., 2008; Beyer et al., 2008). Mice were given a lethal dose of pentobarbital (50 mg/mouse IP). Thoracic aorta was removed and placed in oxygenated Krebs buffer, dissected free of adventitial fat, and cut into 4 segments 4–5 mm in length. Where necessary the endothelial cell layer was removed by rubbing the lumen with a trimmed wooden toothpick. Aortic rings were suspended in organ baths containing 20 ml Krebs buffer (maintained at 37°C and 95% O_2/5% CO_2), connected to a force transducer to measure isometric tension, resting tension was set to 0.5g, and were equilibrated for 45 min. Contraction was recorded for ET-1 (0.1–100 nmol/L), 5-HT (0.01–30 μmol/L), PE (0.01–30 μmol/L), $PGF_{2\alpha}$ (0.1–30 μmol/L), and KCl (10–100 mmol/L). Relaxation was recorded for Ach (0.01–30 μmol/L), SNP (1–10,000 nmol/L) after initial submaximal pre-contraction (40–50% of max) with $PGF_{2\alpha}$. In some experiments, two aortic rings were pre-incubated (30 min) with the drug, while two other segments were untreated. These include 100 μmol/L L-NAME, 1 μmol/L Y-27632, and 10 μmol/L Tempol. For studies on Ca^{2+} sensitivity, aortic rings were equilibrated, then switched to Ca^{2+}-free Krebs buffer with three washes over a period of 15 min. Vessels were then treated with 3 μmol/L ionomycin (in DMSO) for 30 min. Contractile responses were recorded for $CaCl_2$ (0.01 μmol/L–100 mmol/L in Ca^{2+}-free Krebs). For experiments using MLN4924, aortic rings were incubated in DMEM/F12 (16 hr or 6 day;

NIH-PA Author Manuscript

NIH-PA Author Manuscript

NIH-PA Author Manuscript

37°C, 5%CO_2) with either DMSO or 1 μmol/L MLN4924 (in DMSO) prior to preparation onto wire myograph. DMSO or 1 μmol/L MLN4924 was continuously applied to organ baths after each wash during equilibration and throughout the length of the tension studies. Data were collected with PowerLab/8SP and analyzed with Chart 5 software (AD Instruments).

Blood Pressure Analysis

First, S-P467L and NT mice 5–6 months of age were anesthetized with pentobarbital (60 mg/kg intraperitoneally), and cannulation of the carotid artery and jugular vein with 0.040 O.D. sterile tubing was performed. Acute blood pressure responses were measured during anesthesia. Depressor effects were measured in response to Y-27632 (0.1–10 mg/kg through the venous catheter). Data were collected with PowerLab/8SP and analyzed with Chart 5 software (AD Instruments). Second, blood pressure was measured by radiotelemetry as described (Beyer et al., 2008; Halabi et al., 2008). After 7 days of recovery, arterial pressure, heart rate and activity were continuously recorded (sampling every 5 minutes for 20-second intervals). Baseline blood pressure was measured for 7 days. At the beginning of the light phase, mice began continuous treatment with MLN4924 (in 10% hydroxy-propyl-β-cyclodextrin) by subcutaneous injections (30 mg/kg TID), and blood pressure was recorded and analyzed over the next 60 hr (2.5 days). Data were collected and stored using Dataquest ART. Mice were sacrificed at 1 hr following the final injection at 72 hr (3 days). Cheek puncture blood samples were collected and analyzed using i-STAT system CG4+ and CHEM8+ cartridges. Aortic tissue was harvested for protein analyses.

Cell Culture, siRNA Gene Silencing and Western Blotting

Primary smooth muscle cells were isolated from thoracic aorta of S-P467L or NT mice. They were dissected free of perivascular fat, cut into small pieces and dissociated with collagenase, elastase, soybean trypsin inhibitor, and bovine serum albumin type I at 37°C for 30 min. The suspension was centrifuged at 2000 rpm for 5 min, the pellet re-suspended, and cells were plated and maintained in DMEM with 10% FBS, 100 U/ml penicillin and 100 μg/ml streptomycin at 37°C and 5% CO_2. The medium was replaced every 48 hr. Once confluent, the cells were passaged and verified as smooth muscle by staining with α-actin and calponin. Sub-confluent smooth muscle cells at passages 2–4 were used for experiments. Primary culture of aortic smooth muscle cells from Sprague Dawley rat was a gift from Dr. Amy Banes-Berceli (Oakland University, MI). Rat aortic smooth muscle cells were maintained in low glucose (1 g/L) DMEM with 10% FBS, 100 U/ml penicillin and 100 μg/ml streptomycin and kept at 37°C and 5% CO_2. Cells were cultured one day prior to transfection with 20 nmol/L negative control NC1 siRNA or siRNA duplexes targeted to rat Cullin-3 or RhoBTB1 (Integrated DNA Technologies; Coralville, IA) using Hiperfect (Qiagen) using the manufacturer's protocol. Cells were harvested 72 hr later and total protein lysates were stored at −80°C. Rat aortic smooth muscle cells were treated with MLN4924 (1 μmol/L) for 2, 4, 8, 16 and 24 hr or vehicle control (DMSO) for 24 hr and harvested for total protein lysates. Experimental procedures for tissue preparation, transfections, immunoprecipitation, Western Blotting and the antibodies used are described in detail in the Supplemental Experimental Procedures.

Rho-kinase and Rho GTPase Pull-Down Assay

Rho-kinase-dependent phosphorylation of its substrate MYPT1 was measured in aorta and primary aortic smooth muscle cells by ELISA and Rho GTPase activity was determined by pull-down for the active GTP-bound forms of RhoA, Rac1 or Cdc42. The assays are described in detail in the Supplemental Experimental Procedures.

NIH-PA Author Manuscript

NIH-PA Author Manuscript

NIH-PA Author Manuscript

Real-Time RT-PCR, Microarray Analysis, and Chromatin Immunoprecipitation

Real-time PCR (qPCR) analysis was performed using TaqMan Gene Expression Assays. Two independent microarray experiments (series accession, GSE37196) were performed using different array platforms: the Affymetrix mouse genome 2.0 array and the Affymetrix mouse exon 1.0 ST array. Chromatin immunoprecipitation was performed on differentiated 3T3-L1 cells. The experimental procedures for these analyses are described in detail in the Supplemental Experimental Procedures.

Drugs and Reagents

Ach, SNP, KCl, 5-HT, PE, and Nω-Nitro-L-arginine methyl ester (L-NAME) were obtained from Sigma; $PGF_{2\alpha}$ from Pfizer; and Y-27632 from Calbiochem; all of these reagents were dissolved in saline. ET-1 was obtained from Peninsula Laboratories Inc. and dissolved in water. MLN4924 (ActiveBiochem), ionomycin (Calbiochem), Bay K8644 (Sigma) and Phorbol 12,13-dibutryate (Sigma) were dissolved in DMSO.

Statistical Analyses

All data are expressed as mean ± SEM. Data were analyzed with 1- or 2-way analysis of variance (ANOVA, repeated measures when appropriate) using Tukey or Bonferroni post hoc tests. Data sets failing normality or equal variance assumptions, or with small n ($n<5$), were analyzed using non-parametric comparisons (Friedman's ANOVA or Mann-Whitney U Test). $P<0.05$ was considered statistically significant.

Supplementary Material

Refer to Web version on PubMed Central for supplementary material.

Acknowledgments

The authors would like to thank Deborah R. Davis and Maria Alicia Carillo-Sepulveda for assistance and input on this project. We also thank Norma Sinclair, JoAnne Schwarting, and Patricia Yarolem for genotyping mice. Transgenic mice were generated at the University of Iowa Transgenic Animal Facility supported in part by grants from the NIH and from the Roy J. and Lucille A. Carver College of Medicine.

Sources of Funding: This work was supported through research grants from the NIH to CDS (HL084207, HL048058, HL061446, HL062984 and NS024621), to FMF (HL038901, HL062984 and NS024621) and to JLG (HL098276), and from the American Heart Association to PK (11POST5720021) and CJP (10PRE3740029). The authors also gratefully acknowledge the generous research support of the Roy J. Carver Trust.

References

Barroso I, Gurnell M, Crowley VE, Agostini M, Schwabe JW, Soos MA, Maslen GL, Williams TD, Lewis H, Schafer AJ, Chatterjee VK, O'Rahilly S. Dominant negative mutations in human PPARgamma associated with severe insulin resistance, diabetes mellitus and hypertension. Nature. 1999; 402:880–883. [PubMed: 10622252]

Beder LB, Gunduz M, Ouchida M, Gunduz E, Sakai A, Fukushima K, Nagatsuka H, Ito S, Honjo N, Nishizaki K, Shimizu K. Identification of a candidate tumor suppressor gene RHOBTB1 located at a novel allelic loss region 10q21 in head and neck cancer. J Cancer Res Clin Oncol. 2006; 132:19–27. [PubMed: 16170569]

Berthold J, Schenkova K, Ramos S, Miura Y, Furukawa M, Aspenstrom P, Rivero F. Characterization of RhoBTB-dependent Cul3 ubiquitin ligase complexes--evidence for an autoregulatory mechanism. Exp Cell Res. 2008; 314:3453–3465. [PubMed: 18835386]

Beyer AM, de Lange WJ, Halabi CM, Modrick ML, Keen HL, Faraci FM, Sigmund CD. Endothelium-specific interference with peroxisome proliferator activated receptor gamma causes cerebral

NIH-PA Author Manuscript

NIH-PA Author Manuscript

NIH-PA Author Manuscript

vascular dysfunction in response to a high-fat diet. Circ Res. 2008; 103:654–661. [PubMed: 18676352]

Boyden LM, Choi M, Choate KA, Nelson-Williams CJ, Farhi A, Toka HR, Tikhonova IR, Bjornson R, Mane SM, Colussi G, et al. Mutations in kelch-like 3 and cullin 3 cause hypertension and electrolyte abnormalities. Nature. 2012; 482:98–102. [PubMed: 22266938]

Budzyn K, Marley PD, Sobey CG. Targeting Rho and Rho-kinase in the treatment of cardiovascular disease. Trends Pharmacol Sci. 2006; 27:97–104. [PubMed: 16376997]

Chang L, Villacorta L, Zhang J, Garcia-Barrio MT, Yang K, Hamblin M, Whitesall SE, D'Alecy LG, Chen YE. Vascular smooth muscle cell-selective peroxisome proliferator-activated receptor-gamma deletion leads to hypotension. Circulation. 2009; 119:2161–2169. [PubMed: 19364979]

Chen Y, Yang Z, Meng M, Zhao Y, Dong N, Yan H, Liu L, Ding M, Peng HB, Shao F. Cullin mediates degradation of RhoA through evolutionarily conserved BTB adaptors to control actin cytoskeleton structure and cell movement. Mol Cell. 2009; 35:841–855. [PubMed: 19782033]

Chew EH, Poobalasingam T, Hawkey CJ, Hagen T. Characterization of cullin-based E3 ubiquitin ligases in intact mammalian cells--evidence for cullin dimerization. Cell Signal. 2007; 19:1071–1080. [PubMed: 17254749]

Chitaley K, Webb RC. Nitric oxide induces dilation of rat aorta via inhibition of rho-kinase signaling. Hypertension. 2002; 39:438–442. [PubMed: 11882586]

Choi JH, Banks AS, Kamenecka TM, Busby SA, Chalmers MJ, Kumar N, Kuruvilla DS, Shin Y, He Y, Bruning JB, et al. Antidiabetic actions of a non-agonist PPARgamma ligand blocking Cdk5-mediated phosphorylation. Nature. 2011; 477:477–481. [PubMed: 21892191]

Diep QN, El Mabrouk M, Cohn JS, Endemann D, Amiri F, Virdis A, Neves MF, Schiffrin EL. Structure, endothelial function, cell growth, and inflammation in blood vessels of angiotensin II-infused rats: role of peroxisome proliferator-activated receptor-gamma. Circulation. 2002; 105:2296–2302. [PubMed: 12010913]

Dill J, Patel AR, Yang XL, Bachoo R, Powell CM, Li S. A molecular mechanism for ibuprofen-mediated RhoA inhibition in neurons. J Neurosci. 2010; 30:963–972. [PubMed: 20089905]

Graham DJ, Ouellet-Hellstrom R, MaCurdy TE, Ali F, Sholley C, Worrall C, Kelman JA. Risk of acute myocardial infarction, stroke, heart failure, and death in elderly Medicare patients treated with rosiglitazone or pioglitazone. JAMA. 2010; 304:411–418. [PubMed: 20584880]

Gronemeyer H, Gustafsson JA, Laudet V. Principles for modulation of the nuclear receptor superfamily. Nat Rev Drug Discov. 2004; 3:950–964. [PubMed: 15520817]

Halabi CM, Beyer AM, de Lange WJ, Keen HL, Baumbach GL, Faraci FM, Sigmund CD. Interference with PPARg Function in Smooth Muscle Causes Vascular Dysfunction and Hypertension. Cell Metabolism. 2008; 7:215–226. [PubMed: 18316027]

Halabi CM, Sigmund CD. Peroxisome proliferator-activated receptor-gamma and its agonists in hypertension and atherosclerosis: mechanisms and clinical implications. Am J Cardiovasc Drugs. 2005; 5:389–398. [PubMed: 16259527]

Jin L, Ying Z, Hilgers RH, Yin J, Zhao X, Imig JD, Webb RC. Increased RhoA/Rho-kinase signaling mediates spontaneous tone in aorta from angiotensin II-induced hypertensive rats. J Pharmacol Exp Ther. 2006; 318:288–295. [PubMed: 16569756]

Keen HL, Halabi CM, Beyer AM, de Lange WJ, Liu X, Maeda N, Faraci FM, Casavant TL, Sigmund CD. Bioinformatic analysis of gene sets regulated by ligand-activated and dominant-negative peroxisome proliferator-activated receptor gamma in mouse aorta. Arterioscler Thromb Vasc Biol. 2010; 30:518–525. [PubMed: 20018933]

Keen HL, Ryan MJ, Beyer A, Mathur S, Scheetz TE, Gackle BD, Faraci FM, Casavant TL, Sigmund CD. Gene expression profiling of potential PPAR{gamma} target genes in mouse aorta. Physiological Genomics. 2004; 18:33–42. [PubMed: 15054141]

Ketsawatsomkron P, Pelham CJ, Groh S, Keen HL, Faraci FM, Sigmund CD. Does peroxisome proliferator-activated receptor-gamma (PPAR gamma) protect from hypertension directly through effects in the vasculature? J Biol Chem. 2010; 285:9311–9316. [PubMed: 20129921]

Kobayashi N, Ohno T, Yoshida K, Fukushima H, Mamada Y, Nomura M, Hirata H, Machida Y, Shinoda M, Suzuki N, Matsuoka H. Cardioprotective mechanism of telmisartan via PPAR-

NIH-PA Author Manuscript

NIH-PA Author Manuscript

NIH-PA Author Manuscript

gamma-eNOS pathway in dahl salt-sensitive hypertensive rats. Am J Hypertens. 2008; 21:576–581. [PubMed: 18437150]

Kossatz U, Breuhahn K, Wolf B, Hardtke-Wolenski M, Wilkens L, Steinemann D, Singer S, Brass F, Kubicka S, Schlegelberger B, et al. The cyclin E regulator cullin 3 prevents mouse hepatic progenitor cells from becoming tumor-initiating cells. J Clin Invest. 2010; 120:3820–3833. [PubMed: 20978349]

Leck YC, Choo YY, Tan CY, Smith PG, Hagen T. Biochemical and cellular effects of inhibiting Nedd8 conjugation. Biochem Biophys Res Commun. 2010; 398:588–593. [PubMed: 20603103]

Lewis JD, Ferrara A, Peng T, Hedderson M, Bilker WB, Quesenberry CP Jr, Vaughn DJ, Nessel L, Selby J, Strom BL. Risk of bladder cancer among diabetic patients treated with pioglitazone: interim report of a longitudinal cohort study. Diabetes Care. 2011; 34:916–922. [PubMed: 21447663]

Li G, Leff T. Altered promoter recycling rates contribute to dominant-negative activity of human peroxisome proliferator-activated receptor-gamma mutations associated with diabetes. Mol Endocrinol. 2007; 21:857–864. [PubMed: 17227883]

Louis-Dit-Picard H, Barc J, Trujillano D, Miserey-Lenkei S, Bouatia-Naji N, Pylypenko O, Beaurain G, Bonnefond A, Sand O, Simian C, et al. KLHL3 mutations cause familial hyperkalemic hypertension by impairing ion transport in the distal nephron. Nat Genet. 2012; 44:456–3. [PubMed: 22406640]

Maguire JJ, Davenport AP. Regulation of vascular reactivity by established and emerging GPCRs. Trends Pharmacol Sci. 2005; 26:448–454. [PubMed: 16054240]

Momotani K, Artamonov MV, Utepbergenov D, Derewenda U, Derewenda ZS, Somlyo AV. p63RhoGEF couples Galpha(q/11)-mediated signaling to Ca2+ sensitization of vascular smooth muscle contractility. Circ Res. 2011; 109:993–1002. [PubMed: 21885830]

Nethe M, Hordijk PL. The role of ubiquitylation and degradation in RhoGTPase signalling. J Cell Sci. 2010; 123:4011–4018. [PubMed: 21084561]

Petroski MD, Deshaies RJ. Function and regulation of cullin-RING ubiquitin ligases. Nat Rev Mol Cell Biol. 2005; 6:9–20. [PubMed: 15688063]

Ramirez SH, Heilman D, Morsey B, Potula R, Haorah J, Persidsky Y. Activation of peroxisome proliferator-activated receptor gamma (PPARgamma) suppresses Rho GTPases in human brain microvascular endothelial cells and inhibits adhesion and transendothelial migration of HIV-1 infected monocytes. J Immunol. 2008; 180:1854–1865. [PubMed: 18209083]

Sakurada S, Okamoto H, Takuwa N, Sugimoto N, Takuwa Y. Rho activation in excitatory agonist-stimulated vascular smooth muscle. Am J Physiol Cell Physiol. 2001; 281:C571–C578. [PubMed: 11443056]

Sakurada S, Takuwa N, Sugimoto N, Wang Y, Seto M, Sasaki Y, Takuwa Y. Ca2+-dependent activation of Rho and Rho kinase in membrane depolarization-induced and receptor stimulation-induced vascular smooth muscle contraction. Circ Res. 2003; 93:548–556. [PubMed: 12919947]

Sauzeau V, Le JH, Cario-Toumaniantz C, Smolenski A, Lohmann SM, Bertoglio J, Chardin P, Pacaud P, Loirand G. Cyclic GMP-dependent protein kinase signaling pathway inhibits RhoA-induced Ca2+ sensitization of contraction in vascular smooth muscle. J Biol Chem. 2000; 275:21722–21729. [PubMed: 10783386]

Savage DB, Tan GD, Acerini CL, Jebb SA, Agostini M, Gurnell M, Williams RL, Umpleby AM, Thomas EL, Bell JD, et al. Human Metabolic Syndrome Resulting From Dominant-Negative Mutations in the Nuclear Receptor Peroxisome Proliferator-Activated Receptor-{gamma}. Diabetes. 2003; 52:910–917. [PubMed: 12663460]

Schenkova K, Lutz J, Kopp M, Ramos S, Rivero F. MUF1/Leucine-Rich Repeat Containing 41 (LRRC41), a Substrate of RhoBTB-Dependent Cullin 3 Ubiquitin Ligase Complexes, Is a Predominantly Nuclear Dimeric Protein. J Mol Biol. 2012

Sigmund CD. Endothelial and vascular muscle PPARgamma in arterial pressure regulation: lessons from genetic interference and deficiency. Hypertension. 2010; 55:437–444. [PubMed: 20038751]

Smith MA, Maris JM, Gorlick R, Kolb EA, Lock R, Carol H, Keir ST, Reynolds CP, Kang MH, Morton CL, et al. Initial testing of the investigational NEDD8-activating enzyme inhibitor

NIH-PA Author Manuscript

NIH-PA Author Manuscript

NIH-PA Author Manuscript

MLN4924 by the pediatric preclinical testing program. Pediatr Blood Cancer. 2012; 59:246–253. [PubMed: 22012946]

Soucy TA, Smith PG, Milhollen MA, Berger AJ, Gavin JM, Adhikari S, Brownell JE, Burke KE, Cardin DP, Critchley S, et al. An inhibitor of NEDD8-activating enzyme as a new approach to treat cancer. Nature. 2009; 458:732–736. [PubMed: 19360080]

Toriumi Y, Hiraoka M, Watanabe M, Yoshida M. Pioglitazone reduces monocyte adhesion to vascular endothelium under flow by modulating RhoA GTPase and focal adhesion kinase. FEBS Lett. 2003; 553:419–422. [PubMed: 14572662]

Tsai YS, Kim HJ, Takahashi N, Kim HS, Hagaman JR, Kim JK, Maeda N. Hypertension and abnormal fat distribution but not insulin resistance in mice with P465L PPARgamma. J Clin Invest. 2004; 114:240–249. [PubMed: 15254591]

Wakino S, Hayashi K, Kanda T, Tatematsu S, Homma K, Yoshioka K, Takamatsu I, Saruta T. Peroxisome proliferator-activated receptor gamma ligands inhibit Rho/Rho kinase pathway by inducing protein tyrosine phosphatase SHP-2. Circ Res. 2004; 95:e45–e55. [PubMed: 15308580]

Wirth A, Benyo Z, Lukasova M, Leutgeb B, Wettschureck N, Gorbey S, Orsy P, Horvath B, Maser-Gluth C, Greiner E, et al. G12-G13-LARG-mediated signaling in vascular smooth muscle is required for salt-induced hypertension. Nat Med. 2008; 14:64–68. [PubMed: 18084302]

Wu JT, Lin HC, Hu YC, Chien CT. Neddylation and deneddylation regulate Cul1 and Cul3 protein accumulation. Nat Cell Biol. 2005; 7:1014–1020. [PubMed: 16127432]

NIH-PA Author Manuscript

NIH-PA Author Manuscript

NIH-PA Author Manuscript

Research Highlights

- Interference with PPARγ in smooth muscle increases RhoA/Rho-kinase activity.
- RhoBTB1 is a PPARγ target gene which acts in concert with Cullin-3.
- Knockdown of Cullin-3 or inhibition of cullin-RING ligase activity increases RhoA.
- Cullin-RING ligase inhibition increases vascular contraction and arterial pressure.

NIH-PA Author Manuscript

NIH-PA Author Manuscript

NIH-PA Author Manuscript

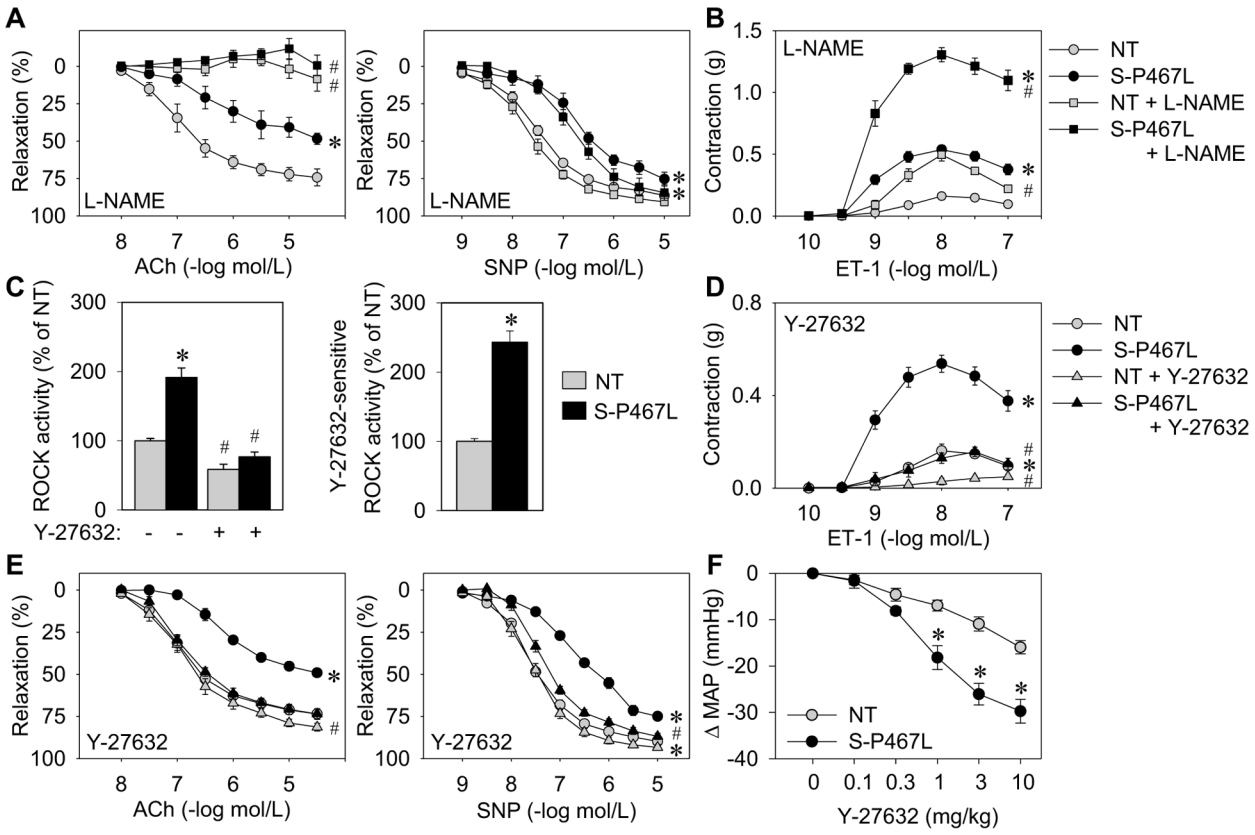

Figure 1. Interference with PPARγ causes increased Rho-kinase activity

Isometric tension was measured on aortic rings from S-P467L (black) and NT littermates (grey). (A–B) Dose-dependent relaxation (following pre-contraction with prostaglandin $F_{2\alpha}$ ($PGF_{2\alpha}$)) in response to acetylcholine (Ach) and sodium nitroprusside (SNP) (A), contraction in response to endothelin 1 (ET-1) (B) was recorded in the absence or presence of NOS inhibitor (30 min pre-incubation; L-NAME, 100 μmol/L) (n=6–12). (C) ELISA of phospho-Thr^{696} MYPT1 subunit of MLCP in the absence or presence of Rho-kinase inhibitor (Y-27632) using aortic tissue from NT and S-P467L mice (n=4–9) and quantification of Y-27632-sensitive Rho-kinase activity. (D–E) Effect of Rho-kinase inhibition (30 min pre-incubation; Y-27632, 1 μmol/L) on contraction or relaxation of aortic rings from S-P467L and NT mice in response to ET-1 (D) or Ach and SNP (E) (n=9–12). (F) Direct blood pressure measurements were recorded in response to acute intravenous injection of the Rho-kinase inhibitor Y-27632 in anesthetized NT and S-P467L mice (n=6). See also Figures S1 and S2. * $p<0.05$ S-P467L vs. NT. # $p<0.05$ treated vs. non-treated. Error bars represent SEM.

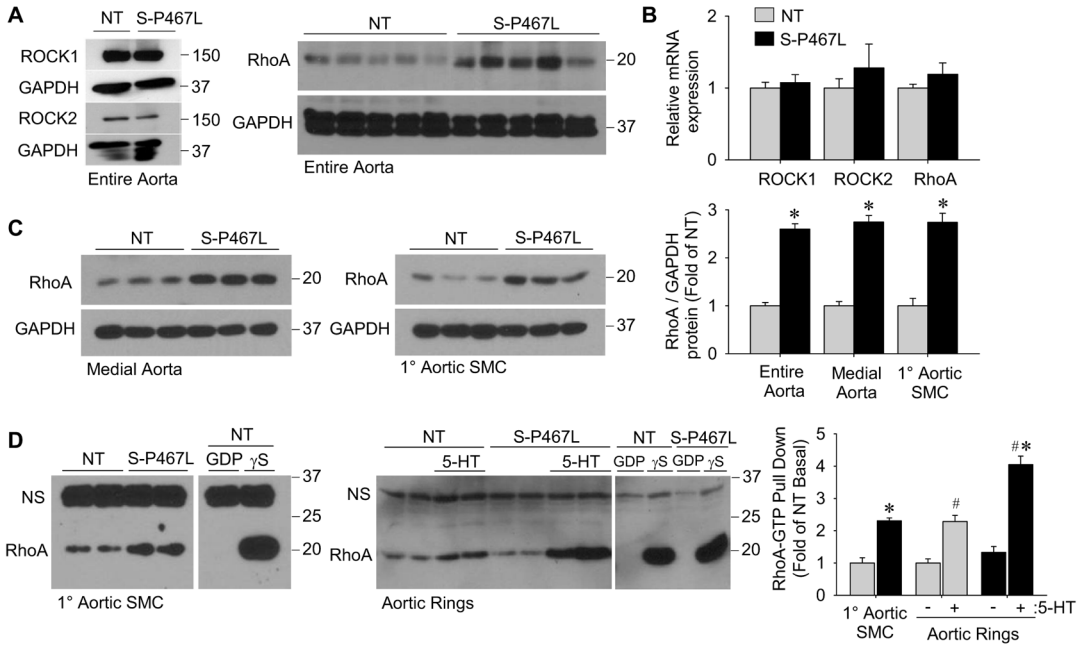

Figure 2. Increased RhoA protein expression and activity

(A) Protein levels of ROCK1 and ROCK2 (n=4–5) or RhoA (n=8) in entire aorta of NT and S-P467L mice determined by Western blot. (B) Expression of ROCK1, ROCK2 and RhoA mRNA in aortic tissue determined by qPCR (n=10–11). (C) Total RhoA protein levels in medial aorta (dissected free of endothelium and adventitia) (n=8) or 1° aortic smooth muscle cells (SMC) (n=6) determined by Western blot and quantification. (D) Western blot of RhoA-GTP pull-down using non-treated 1° aortic SMC from NT and S-P467L mice (n=4), and aortic rings equilibrated to 0.5 g tension plus or minus agonist-stimulation by 5-HT (1 μmol/L, 5 min) (n=4) and quantification. “NS” indicates non-specific band. See also Figure S3. * $p<0.05$ S-P467L vs. NT. # $p < 0.05$ treated vs. non-treated. Error bars represent SEM.

NIH-PA Author Manuscript NIH-PA Author Manuscript NIH-PA Author Manuscript

NIH-PA Author Manuscript

NIH-PA Author Manuscript

NIH-PA Author Manuscript

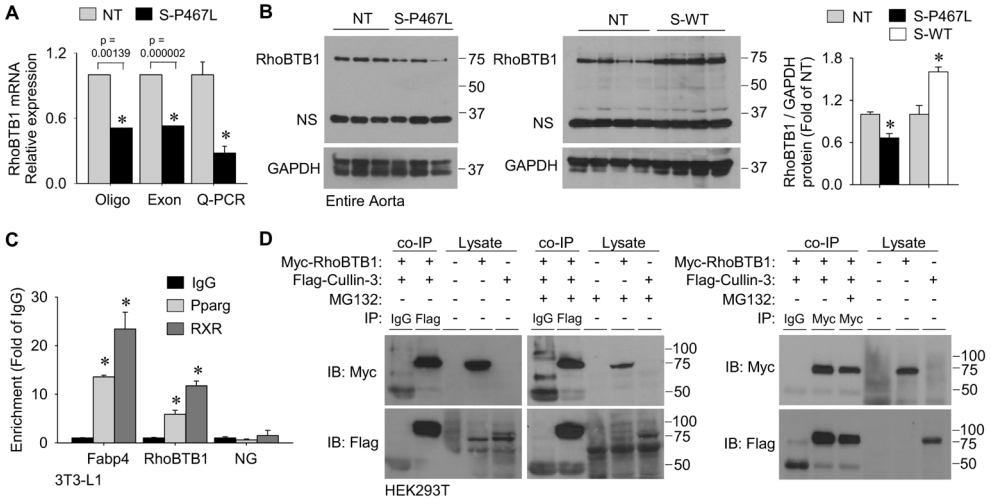

Figure 3. Identification of the Cullin-3 interacting protein RhoBTB1 as a PPARγ target gene

(A) Relative mRNA expression of RhoBTB1 in aortic tissue from S-P467L mice relative to NT littermates in two independent microarray experiments using different array platforms and validation by Q-PCR (n=10–11). Oligo array refers to the Affymetrix mouse genome 2.0 array (probe set 1429656_at, n=2 for NT and n=3 for S-P467L) and Exon array refers to the Affymetrix mouse exon 1.0 ST array (probe set 6768601, n=5 for NT and n=7 for S-P467L). (B) Western blot for RhoBTB1protein expression in aorta from S-P467L and littermate NT mice (n=8) or from S-WT and littermate NT mice (n=4) and quantification. "NS" indicates non-specific band. (C) Validation of PPARγ and RXR binding at FABP4 and RhoBTB1 PPREs by ChIP from duplicate experiments. Data is displayed as the fold enrichment relative to the IgG signal at the region of interest (* $p<0.05$ Pparg or RXR vs. IgG). NG represents a non-specific region of the genome which does not contain any known PPRE sequences. (D) Immunoprecipitation (IP) experiments using HEK293T cells transfected with plasmids expressing Myc-RhoBTB1, Flag-Cullin-3 or both. The antisera used for each IP is indicated. Lysates indicate samples not subjected to IP as controls for antisera specificity. Cells were treated with either MG132 (5 μmol/L) or vehicle (DMSO). The left blots are representative of n=4, and the right blot was representative of duplicate experiments. See also Figure S4. * $p<0.05$ S-P467L or S-WT vs. NT. Error bars represent SEM.

NIH-PA Author Manuscript
NIH-PA Author Manuscript
NIH-PA Author Manuscript

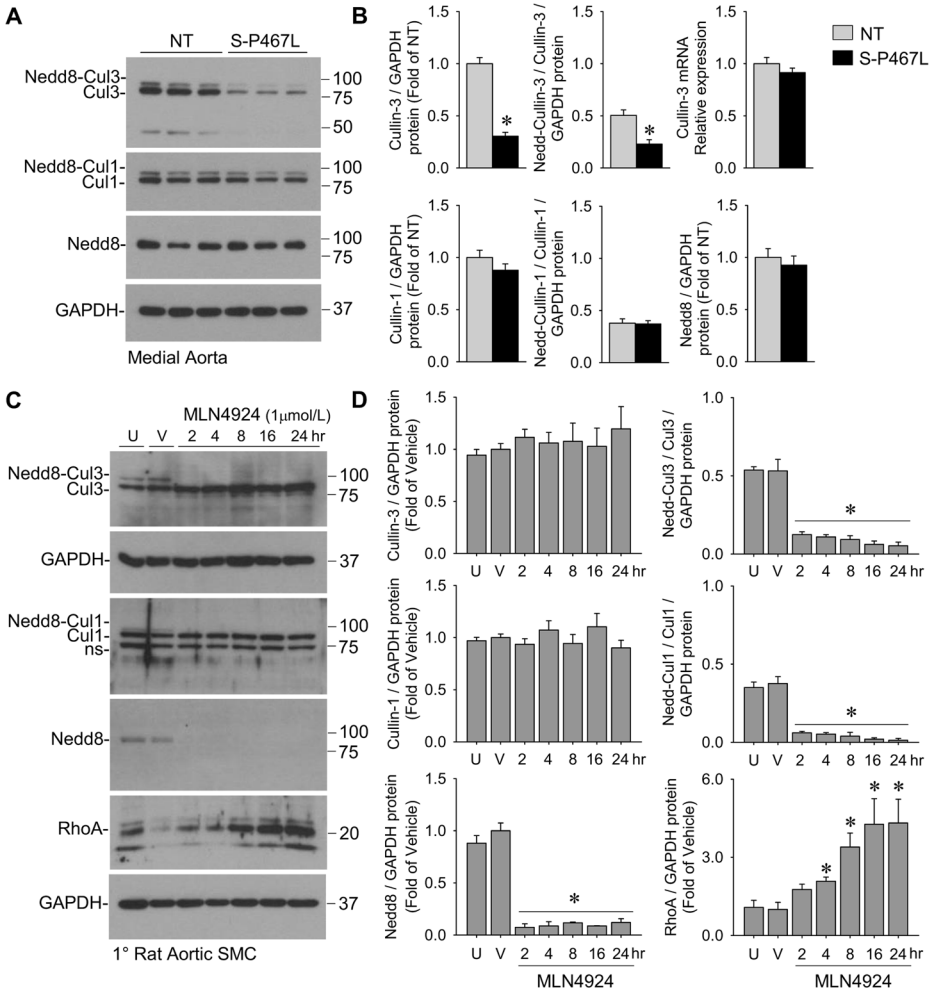

Figure 4. Interference with PPARγ causes decreased Cullin-3 and Nedd8-Cullin-3

(A–B) Protein levels of Cullin-3 and neddylated Cullin-3, Cullin-1 and neddylated Cullin-1, and total Nedd8-conjugates (Nedd8) in medial aortic tissue from S-P467L and NT mice determined by Western blot (n=8–9) and their quantification. Neddylation is the covalent attachment of Nedd8 onto a target protein. The lower molecular weight band of the doublet (~85 kDa) is unneddylated Cullin-3 or Cullin-1 (denoted as Cul3 or Cul1) whereas the higher band (~95 kDa) is the neddylated Cullin-3 or Cullin-1 product (denoted as Nedd8-Cul3 or Nedd8-Cul1). Cullin-3 mRNA expression determined by qPCR (n=10). See also Table S1. * $p<0.05$ S-P467L vs. NT. Error bars represent SEM. (C–D) Primary rat aortic smooth muscle cells treated with the Nedd8-activating enzyme inhibitor MLN4924 (1 μmol/L) or DMSO over a time-course of 24 hr. Protein lysates were assessed for Cullin-3, Cullin-1, Nedd8 and RhoA by Western blot and quantified (n=4). U, untreated; V, vehicle (DMSO, 24 hr). "NS" indicates non-specific band. * $p<0.05$ MLN4924-treated vs. vehicle-treated. Error bars represent SEM.

NIH-PA Author Manuscript

NIH-PA Author Manuscript

NIH-PA Author Manuscript

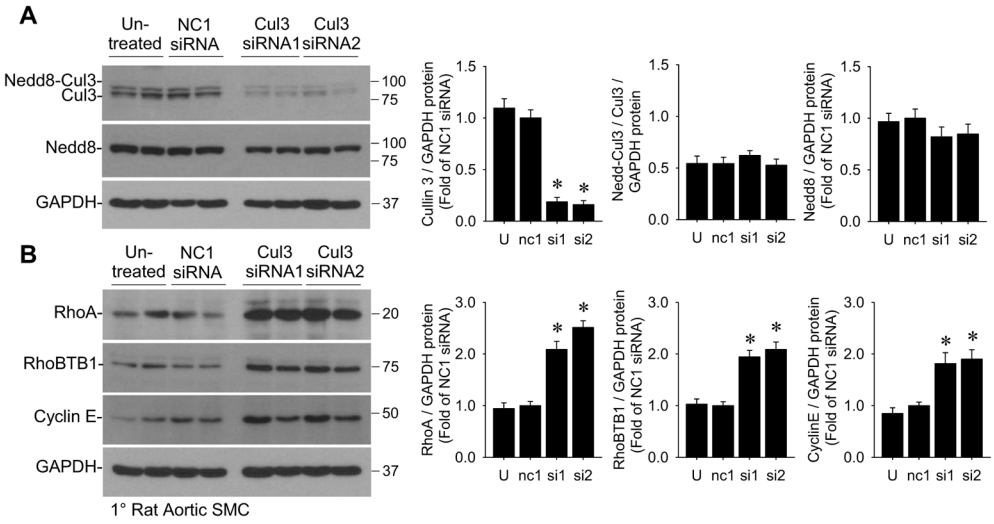

Figure 5. siRNA-knockdown of Cullin-3 increases RhoA in rat aortic smooth muscle cells

(A–B) 1° rat aortic SMC treated with negative contr ol siRNA (NC1) or two different siRNAs targeting Cullin-3 were assessed for protein levels of Cullin-3 and total Nedd8-conjugates (Nedd8) (A) and Cullin-3 substrates RhoA, RhoBTB1, and Cyclin E (B) by Western blot (n=6). U, untreated; nc1, negative control siRNA; si1, Cullin-3 siRNA #1; si2, Cullin-3 siRNA #2. * $p<0.05$ Cullin-3 siRNA-treated vs. NC1 siRNA-treated. Error bars represent SEM.

NIH-PA Author Manuscript

NIH-PA Author Manuscript

NIH-PA Author Manuscript

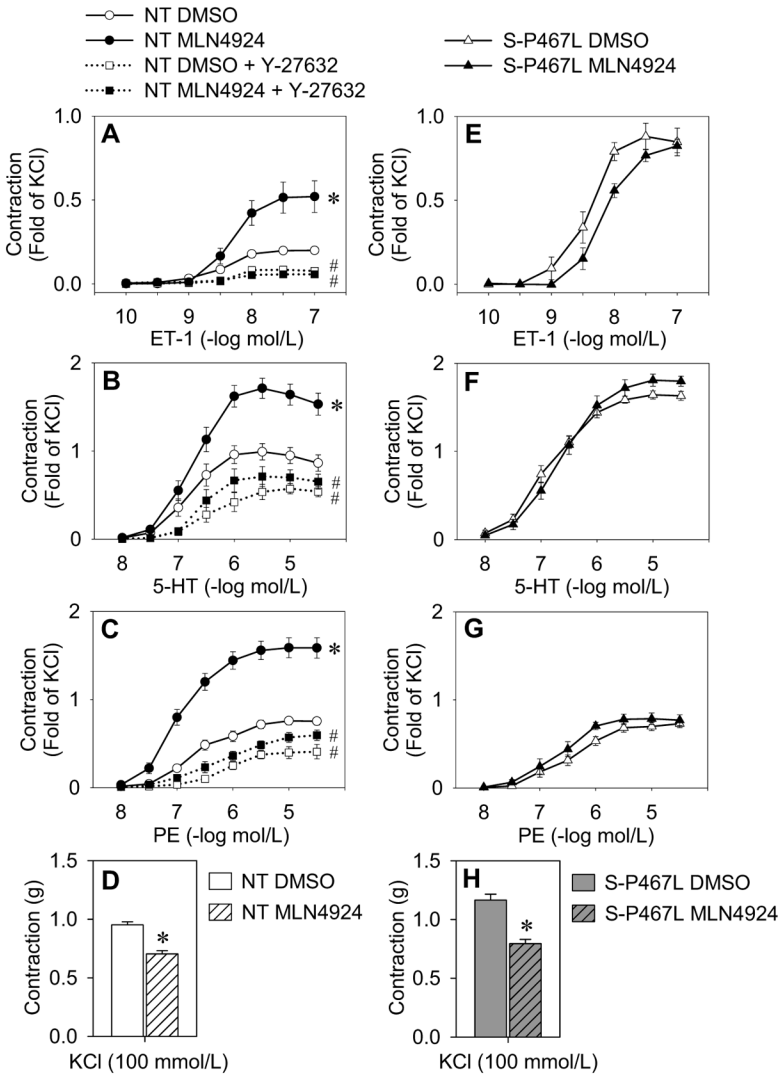

Figure 6. Inhibition of total cullin activity enhances agonist-mediated contraction

(A–H) Isometric tension data on aortic rings from NT mice (A–D; n=10) or S-P467L mice (E–H; n=6) incubated in DMEM/F12 (37°C, 5%CO_2) with DMSO or MLN4924 (1 μmol/L) for 16 hr. DMSO and MLN4924 were continuously applied throughout the tension experiments. Contractile responses were recorded to ET-1 (A and E), 5-HT (B and F), phenylephrine (PE) (C and G) or KCl (D and H). Aortic rings from NT mice (A–D) were further studied in the absence or presence of Rho-kinase inhibitor (30 min pre-incubation; Y-27632, 1 μmol/L) (n=6). Data are normalized to maximum contraction (fold of 100 mmol/L KCl). * $p<0.05$ MLN4924-treated vs. vehicle-treated. # $p<0.05$ Y-27632-treated vs. MLN4924- or vehicle-treated alone. Error bars represent SEM.

NIH-PA Author Manuscript

NIH-PA Author Manuscript

NIH-PA Author Manuscript

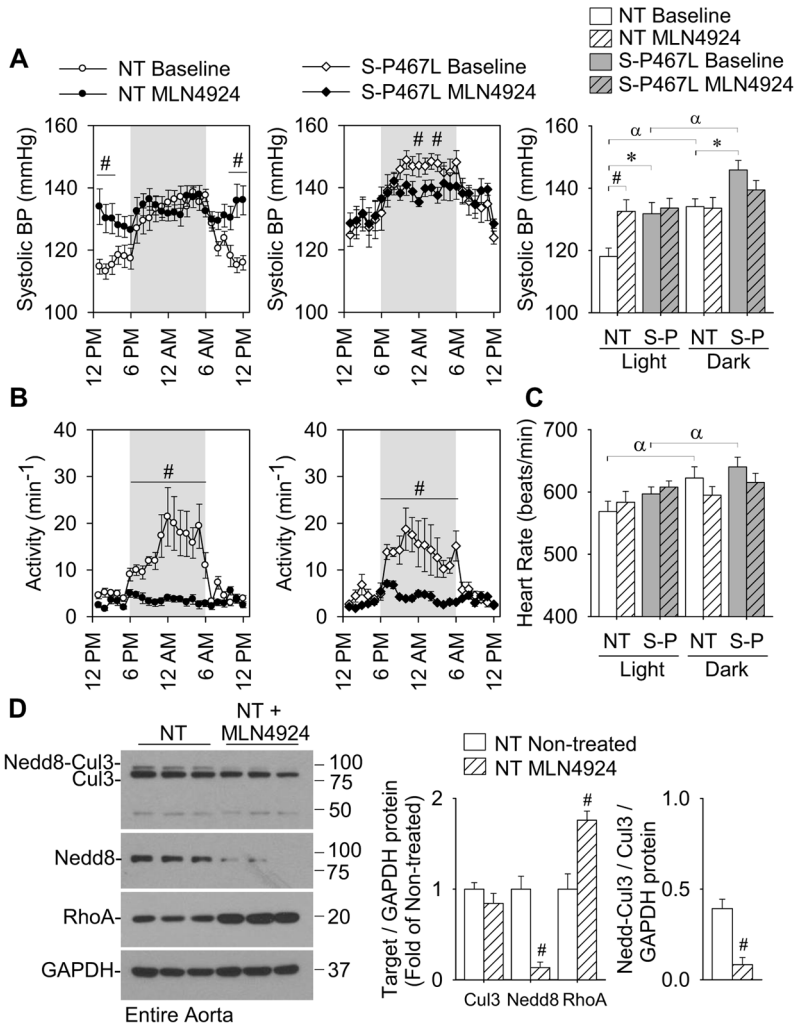

Figure 7. Inhibition of total cullin activity increases daytime blood pressure in normal mice

(A–C) Systolic blood pressure (A), spontaneous activity (B) and heart rate (C) recorded continuously throughout the light:dark cycle by radiotelemetry in NT (n=9) and S-P467L mice (n=7). Baseline measurements were taken for 7 days. At the beginning of the light phase, mice began continuous dosing with MLN4924 (subcutaneous injections; 30 mg/kg TID). Data represent the average of the baseline measurements (7 days) and the average of MLN4924 treatment over 2.5 days (60 hr). See also Figure S5 and Table S2. # $p<0.05$ MLN4924-treatment vs. baseline. * $p<0.05$ S-P467L vs. NT. α $p<0.05$ dark cycle vs. light cycle. Error bars represent SEM.